PAPER • OPEN ACCESS

Beam Coupling Impedance Contribution of Flange Aperture Gaps: a Numerical Study for Elettra 2.0

To cite this article: S. Cleva *et al* 2024 *J. Phys.: Conf. Ser.* **2687** 062015

View the article online for updates and enhancements.

You may also like

Beam Coupling Impedance Contribution of Flange Aperture Gaps: a Numerical Study for Elettra 2.0

S. Cleva[1,a,*]**, I. Cudin**[1,b]**, E. Karantzoulis**[1,c]**, L. Rumiz**[1,d]**,
M. Comisso**[2,e] **and A. Passarelli**[3,f]

[1]Elettra Sincrotrone Trieste, Area Science Park, 34149 Basovizza, Trieste, Italy
[2]Department of Engineering and Architecture (DIA), University of Trieste,34127 Trieste, Italy
[3]INFN Naples Unit, Via Cintia, 80126 Napoli, Italy

E-mail: [a]stefano.cleva@elettra.eu; [b]ivan.cudin@elettra.eu;
[c]emanuel.karantzoulis@elettra.eu; [d]luca.rumiz@elettra.eu; [e]mcomisso@units.it;
[f]andrea.passarelli@na.infn.it

[*]Corresponding author

Abstract.   The accurate analysis of any possible source of beam instability is mandatory for the design of a new particle accelerator, especially for high-current and ultra-low emittance synchrotrons. In the specific case of instabilities driven by the coupling between the charged particle beam and the electromagnetic field excited by the beam itself, the corresponding effect is estimated through the beam coupling impedance. The modeling of this effect is essential to perform a rigorous evaluation of the coupling impedance budget able to account for all devices present in the entire machine. To deal with this problem, this paper focuses on the estimation of the contribution of the joints lying between the different vacuum chamber sections, by performing a comparative numerical analysis that takes into account different aperture gaps between the flanges. The results point out the criticality of many small-impedance contributions that, added together, must be lower than a predefined impedance threshold.

1. Introduction

Operating for users since 1994, the existing third-generation Italian synchrotron radiation facility Elettra [1] is going to be replaced by Elettra 2.0 [2, 3], an ultra-low emittance light source able to provide ultra-high brilliant and coherent photon beams. To ensure the performance of Elettra 2.0 is not affected by potential sources of beam instability, it is necessary to thoroughly examine the electromagnetic interaction between the circulating beam and its surrounding environment. This interaction can be evaluated through the wake field in the time domain and the beam coupling impedance in the frequency domain [4]. It is important to keep the overall machine impedance below a predetermined threshold to prevent any possible sources of beam instability. This work focuses on estimating the contribution of the joints located between different sections of the vacuum chamber. This problem has also been addressed in other contexts such as CERN-SPS, where RF contacts have been used [5, 6], or PSI-SLS2, where zero gap flanges have been chosen [7]. This paper describes a comparative numerical analysis of the impedance of two types of vacuum flanges, taking into account different gap thicknesses between them. The obtained results are exploited to discuss the impact of the different impedance contributions in the forthcoming development of Elettra 2.0.
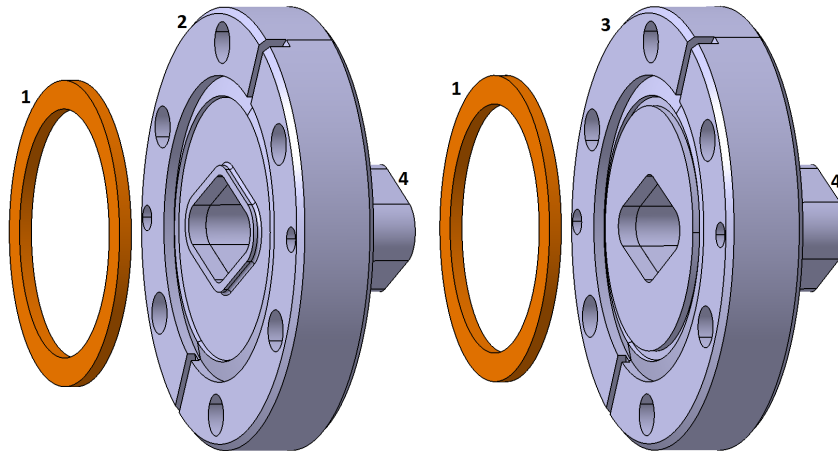
Figure 1. Flanges mechanical drawings. On the left, the SFL type (2) and, on the right, the SFP type (3). Also the gasket (1) and the rhomboidal vacuum pipe (4) are shown.

2. Flange models

Two different types of flanges are considered in this paper. The first one is a Spigot Flange Lip (SFL) type, while the second one is a Spigot Flange Planar (SFP) type.

2.1. Mechanical model

The mechanical drawings of the flanges under evaluation are detailed in Figure 1. The main difference between SFL and SFP types resides in the geometry of the resulting gap that separates the opposite sides of the vacuum joint: in the SFP case, the gap's volume is reduced with respect to the SFP's one. This is the result of the different geometry of the transition between the gasket housing and the rhomboidal vacuum chamber.

2.2. Electromagnetic model

A simplified electromagnetic (EM) model has been derived from the mechanical one to simulate the interaction between the charged particle beam and its surrounding environment by considering the short vacuum pipes, opposite-facing flanges and the gasket. To simplify the structure, only the surfaces, volumes and materials interacting with the EM field of the charged particles beam have been taken into account. The correspondence between the mechanical and EM models is summarized in Table 1.

The basic EM models of the SFP and SFL are shown in Figure 2, where the gasket and the flanges are assumed of the same material being considered as the background material in the model. The gap G and the cavity depth C of the parasitic cavities formed by the opposite sides

Table 1. Correspondence between mechanical and electromagnetic model.

Mechanical	Electromagnetic
inner vacuum volume	inner vacuum volume
materials wall thickness*	background lossy metal
input and output apertures	open boundaries

*The minimum thickness of the conductive materials is 1.5 mm, large enough to guarantee the full electromagnetic field penetration in the conductors due to the skin effect at the considered frequencies.
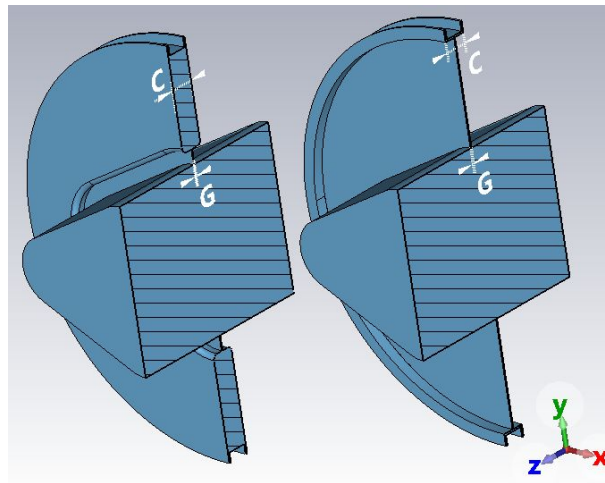
Figure 2. Electromagnetic model of the two flanges: 3D longitudinal cut views. The SFL type (left) and the SFP type (right).

of the flanges are also illustrated. A direct comparison between the two shapes shows that the passive cavity volume of SFL is larger than that of SFP.

3. Electromagnetic simulation

Two sets of EM simulations are carried out resorting to CST Particle Studio by Dassault Systemes Simulia [8]. The first set aims to evaluate and compare the longitudinal impedance of the two types of flanges assuming the nominal geometries, while the second set focuses on the evaluation of the effects determined by the constructive tolerances and the parameter variations.

The transverse symmetry of both types of flanges allows one to exploit the symmetry with respect to the $Y-Z$ and $X-Z$ planes for the boundary conditions, thus enabling to simulate just one-fourth of the actual EM structure. Moreover, in order to find a reasonable trade-off between
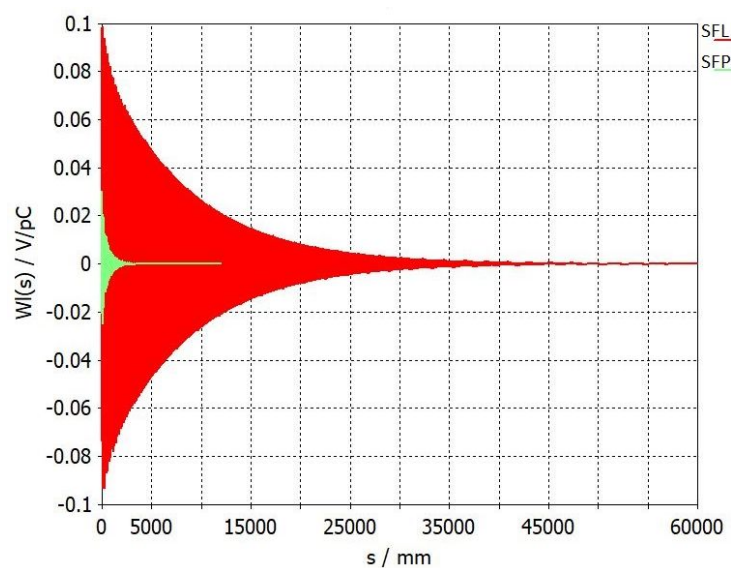

Figure 3. SFL (red) and SFP (green) wake potential comparison.

Table 2. R_s, Q and $\mathrm{Re}(Z/n)$ comparison between the SFL and SFP dominant resonance.

	f_r [GHz]	R_s [Ω]	Q	$\mathrm{Re}(Z/n)$ [Ω]
SFL	2.9388	1247.7	287	0.4914
SFP	4.8793	22.64	56	5.4e-03

the number of mesh cells, the convergence results, and the computational time, a suitable number of preliminary simulations is carried out by varying the mesh density. The large aspect ratio of the flanges under investigation is also implicitly taken into account by maintaining oversized the number of mesh cells.

3.1. Flanges nominal dimensions
The nominal dimensions of the flanges are:

- gap: G = 0.1 mm,
- cavity depth: C = 2.4 mm,
- total longitudinal length: 20 mm,
- cavity main radius (gasket inner radius): 19.6 mm,
- input and output apertures: the same as the rhomboidal vacuum pipe's inner dimensions (27×17 mm).

The relativistic exciting Gaussian beam has bunch length $\sigma = 4$ mm in order to have an impedance estimation up to 25 GHz. The lossy metal considered as background is the AISI 316L stainless steel, with an electric conductivity $\sigma_{316L} = 1.35\mathrm{e}6$ S/m at room temperature. In order to evaluate the longitudinal impedance of both SFL and SFP, the exciting beam and the wakefield integration path are set on the longitudinal z-axis of the simulated structures, and the wake potentials are calculated by the Wakefield solver. In Figure 3 the SFL (red trace) and SFP (green trace) wake potentials appear overlapped.

A first qualitative comparison between the wake potential lengths and initial amplitudes, considered together with the shapes of the parasitic cavities (as depicted in Figure 2), suggests that the SFL cavity has a higher energy storage capability with respect to the SFP one.
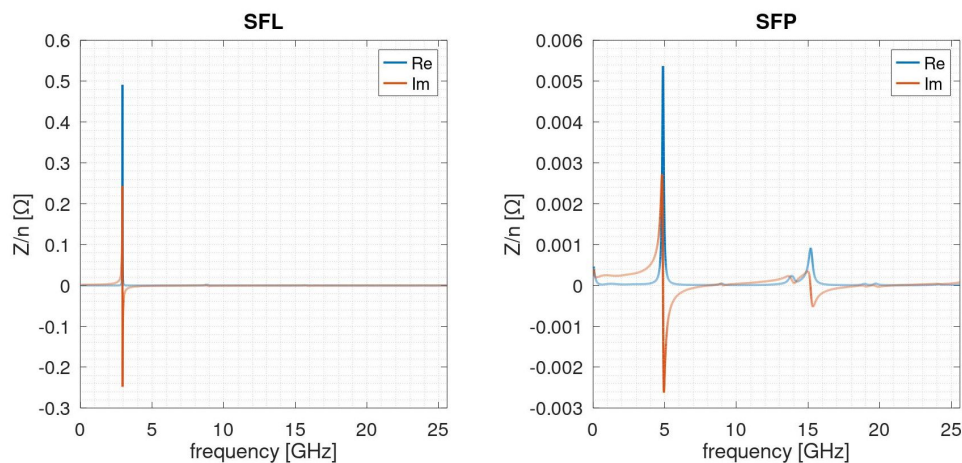

Figure 4. Normalized longitudinal impedance: SFL (left) and SFP (right).

Table 3. Wake loss factor varying the gap G.

| G [mm]	0.1	0.2	0.3	0.4
WLF [e-2V/pC]	1.31	2.48	3.63	4.77

Performing some numerical analyses, both the broadband and narrowband (resonant) impedance contributions can be estimated, thus enabling a quantitative comparison between the SFL and SFP flange behavior in the frequency domain. Each narrowband impedance contribution is characterized by its resonant frequency f_r, its shunt resistance R_s (i.e. the amplitude of the real part of the complex impedance at the resonance frequency), and the quality factor Q. These values are summarized in Table 2 for the main longitudinal resonant mode of the investigated flanges.

The longitudinal analysis is then completed by calculating the normalized longitudinal impedances Z/n [9] (see Figure 4), where $n = f/f_{rev}$ is the mode number, with f_{rev} denoting the revolution frequency of the accelerator. The wake loss factors (WLFs) for SFL and SFP are 4.83e-02V/pC and 1.31e-02V/pC, respectively. A comparison between the real parts of Z/n shows that the SFL type is almost 100 times higher than the SFP one, while the ratio of WLFs is about 3.69.

3.2. Mechanical tolerances and parametric simulations

The previously presented EM analysis on the SFP nominal model has allowed the evaluation of the variations of the longitudinal impedance for different geometric tolerances. Assuming that only one parameter varies at a time, we can now estimate the effects introduced by the manufacturing and assembly tolerances. The considered parameter variations and the corresponding effects can be listed and discussed as follows.

- The expansion of the gap G from 0.1mm to 0.4mm in steps of 0.1mm determines the increase of both the main and secondary peak amplitude of the real part of the longitudinal impedance, with a frequency shift toward higher values (Figure 5). The WLF increases too
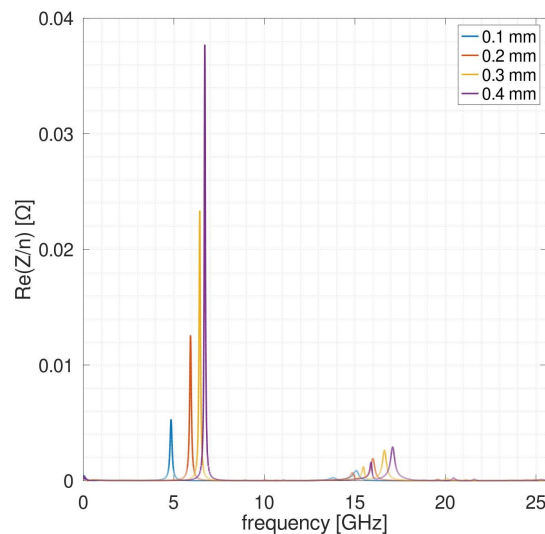
Figure 5. Parametric dependence of Re(Z/n) on G.

(Table 3).

- The increase of the gasket inner radius from 19.6mm to 20.0mm determines the growth of both the main and secondary peak amplitude of the real part of the longitudinal impedance, with a frequency shift toward lower values. The WLF remains constant.

- The increase of the longitudinal length from 10mm to 70mm does not provide appreciable modifications on the real and imaginary part of the longitudinal impedance. This is because of the long range nature of the resonant field trapped in the gap, whose frequency (4.8793GHz) is below the cutoff frequency of the vacuum pipe (7GHz).

4. Conclusion

The longitudinal normalized impedance and the wake loss factor are useful to provide an effective description of the EM interaction between the charged particle beam and its surroundings. Our simulations show that the normalized longitudinal impedance of the SFP flange type is one hundred times lower than that of the SFL one, thus suggesting the opportunity of avoiding the installation of the second flange. Furthermore, thanks to the results of the parametric analysis on the SFP type, we have shown the importance of matching the geometric tolerance limit values for both the gap and the gasket radius. It is worth mentioning that the real part of the impedance is also related to the RF heating, which could represent a serious issue, both in terms of cooling and extra RF power that the accelerating cavities have to deliver to the beam. In the next future, the longitudinal impedance, and consequently the RF heating, of the SFP-based vacuum joints could be further reduced by acting on the beam-flange coupling by:

- optimizing the cavity geometry (lowering Q);
- shielding the cavity aperture (RF fingers for surface currents).

References

[1] Karantzoulis E, Carniel A, and Krecic S 2019 Elettra, present and future *Proc. Int. Particle Accell. Conf. (Melbourne)* (JACoW Publishing, Geneva, Switzerland) p TUPGW031

[2] Karantzoulis E 2018 Elettra 2.0 - The diffraction limited successor of Elettra *Nucl. Instr. Meth. Phys. Res. Sec. A: Accel., Spectrom., Detect. Assoc. Equip.* **880** 158

[3] Karantzoulis E 2023 Elettra 2.0 - Italy's lightsource for science and outreach *Int. Particle Accell. Conf. - Invited Oral Pres. (Venice)*

[4] Palumbo L, Vaccaro V G, and Zobov M 1995 Wake fields and impedance *CAS - CERN Accel. Sch.: Adv. Accel. Phys. Cour.* p 331

[5] Campelo J E 2015 Longitudinal impedance characterization of the CERN SPS vacuum flanges *Proc. Int. Particle Accell. Conf (Richmond)* vol 1 (JACoW Publishing, Geneva, Switzerland) p MOPJE036

[6] Kaltenbacher T and Vollinger C 2017 Characterization of shielding for the CERN-SPS vacuum flangesWith respect to beam coupling impedance *Int. Particle Accell. Conf. (Copenhagen)* (JACoW Publishing, Geneva, Switzerland) p WEPIK090

[7] Braun H, Garvey, T Jorg M, et al. 2021 *SLS 2.0 Storage Ring Tech. Des. Rep.*

[8] Dassault Systémes Simulia 2022 *CST Computer Simulation Technology, Studio Suite*

[9] Wiedemann H 2015 *Particle accelerator physics* (Berlin, Springer)